Spontaneous Squamous Cell Carcinoma Induced by the Somatic Inactivation of *Retinoblastoma* and *Trp53* Tumor Suppressors

Ana Belén Martínez-Cruz, Mirentxu Santos, M. Fernanda Lara, Carmen Segrelles, Sergio Ruiz, Marta Moral, Corina Lorz, Ramón García-Escudero, and Jesús M. Paramio

Molecular Oncology Unit, Division of Biomedicine, Centro de Investigaciones Energéticas, Medioambientales y Tecnológicas, Madrid, Spain

Abstract

Squamous cell carcinomas (SCC) represent the most aggressive type of nonmelanoma skin cancer. Although little is known about the causal alterations of SCCs, in organ-transplanted patients the E7 and E6 oncogenes of human papillomavirus, targeting the p53- and pRb-dependent pathways, have been widely involved. Here, we report the functional consequences of the simultaneous elimination of *Trp53* and *retinoblastoma* (*Rb*) genes in epidermis using Cre-*lox*P system. Loss of p53, but not pRb, produces spontaneous tumor development, indicating that p53 is the predominant tumor suppressor acting in mouse epidermis. Although the simultaneous inactivation of pRb and p53 does not aggravate the phenotype observed in *Rb*-deficient epidermis in terms of proliferation and/or differentiation, spontaneous SCC development is severely accelerated in doubly deficient mice. The tumors are aggressive and undifferentiated and display a hair follicle origin. Detailed analysis indicates that the acceleration is mediated by premature activation of the epidermal growth factor receptor/Akt pathway, resulting in increased proliferation in normal and dysplastic hair follicles and augmented tumor angiogenesis. The molecular characteristics of this model provide valuable tools to understand epidermal tumor formation and may ultimately contribute to the development of therapies for the treatment of aggressive squamous cancer. [Cancer Res 2008;68(3):683–92]

Introduction

The nonmelanoma skin cancer (NMSC), the most common cancer among humans, comprises two major types: squamous cell carcinoma (SCC) and basal cell carcinoma (BCC). Several factors, including the clinical characteristics, differentiate between BCCs and SCCs, being the latter more aggressive with increased metastatic properties. The major factor responsible for development of NMSC is UV radiation (1, 2). However, whereas for BCC development the genetic hallmark is abrogation of the *patched-sonic hedgehog* pathway, little is known about the causal alterations of SCCs. Mutations in *Trp53* tumor suppressor gene are frequently observed in both types of tumors. Interestingly, organ transplant recipients have an up to 100-fold increased risk of SCC and a 10-fold increased risk of BCC, resulting in a reversal of the normal ratio of SCC to BCC (2). Several studies have suggested the involvement of cutaneous human papillomaviruses (HPV) in the development of NMSCs, in part through alterations in p53 and pRb pathways mediated by E6 and E7 oncoproteins, respectively (2).

The *Trp53* gene product, p53, coordinates the cellular response to stress, including DNA damage, hypoxia, and oncogenic stress through transcriptional mechanisms, resulting in cell cycle arrest, senescence, or apoptosis (3). The tumor suppressor *retinoblastoma* (*Rb*) also acts through transcriptional mechanisms to regulate cell cycle progression, differentiation, and apoptosis (4). Numerous evidences have shown the functional connection between pRb- and p53-dependent pathways (5, 6). For instance, $p21^{waf1}$ is induced by p53 and negatively regulates cyclin-dependent kinase (cdk) function, leading to the inhibition of mechanisms that functionally inactivate pRb by phosphorylation. In addition, $p21^{waf1}$ can inhibit cell proliferation in cells lacking pRb through direct binding to cdks and E2F transcription factors (7–9). On the other hand, the inactivation of pRb leads to activation of E2F transcription factors, which produces sustained p53 induction through $p19^{arf}$-dependent (10, 11) and $p19^{arf}$-independent mechanisms (12, 13). In support of these cooperative functions, different transgenic mouse models bearing inactivation of both tumor suppressor genes have been generated, providing useful prototypes of human tumors of lung (14), medulloblastoma (15), and prostate (16).

In epidermis, the specific ablation of *Rb* gene does not result in spontaneous tumors (17), unless other pRb family members, such as p107, are also inactivated (18).[1] In addition, chemical carcinogenesis protocols in these mice result in reduced number of tumors, which also show smaller size and increased malignant conversion (19). This is mediated, at least in part, by the induction of p53 and the consequent apoptosis at early stages (20). Importantly, the subsequent inactivation of p107 abolishes p53-dependent apoptotic processes, leading to spontaneous tumor formation (18).[1] It has been previously reported that the specific ablation of *Trp53* gene in stratified epithelia leads to spontaneous tumor development (21, 22). However, to our knowledge, there are no studies about the possible cooperation between pRb and p53 in epidermis *in vivo*.

To analyze all these aspects, we sought to create a mouse skin cancer model based on joint inactivation of *Rb* and *Trp53* in

Note: Supplementary data for this article are available at Cancer Research Online (http://cancerres.aacrjournals.org/).

A.B. Martínez-Cruz and M. Santos contributed equally to this work.

Current address for S. Ruiz: Centro de Investigación del Cáncer and Instituto de Biología Molecular y Celular del Cáncer, Consejo Superior de Investigaciones Cientificas-University of Salamanca, E-37007 Salamanca, Spain.

Requests for reprints: Jesús M. Paramio, Molecular Oncology Unit, Centro de Investigaciones Energéticas, Medioambientales y Tecnológicas, E-28040 Madrid, Spain. Phone: 34-913460865; Fax: 34-913466484; E-mail: jesusm.paramio@ciemat.es.

doi:10.1158/0008-5472.CAN-07-3049

[1] M.F. Lara et al., in press.

stratified epithelia. To this, we bred mice bearing floxed alleles of *Rb* gene ($Rb^{F19/F19}$; ref. 17) with mice bearing floxed alleles of *Trp53* ($Trp53^{F2/F10}$; refs. 22, 23) and with transgenic K14*cre* mice (22). The $Rb^{F19/F19}$;$Trp53^{F2/F10}$;K14*cre* (thereafter $pRb^{-/-}$;$p53^{-/-}$) mice, losing these tumor suppressor genes in stratified epithelia (17, 22), and their different allelic combinations, were generated. We show that somatic inactivation of *Trp53* does not produce any evident phenotypic changes nor it aggravates the phenotypic consequences of *Rb* ablation in epidermis. On the other hand, p53 loss leads to spontaneous tumor formation, a process that is dramatically accelerated by simultaneous pRb loss. Such cooperative activities seem to be promoted by the early activation of the epidermal growth factor receptor (EGFR)/Akt axis, leading to an early angiogenic response.

Materials and Methods

Experimental mice and genotyping. Mice of the different genotypes in FVB background [$Rb^{F19/F19}$ (17), $Trp53^{F2/F10}$ (22, 23), and K14*cre* mice (22)] were genotyped by PCR using specific primers as previously described (17, 22, 23). Mice of all genotypes were monitored for tumor formation over a period of 20 months. Tumor volume was calculated as $\pi(4/3) \times (\text{width}/2)^2 \times (\text{length}/2)$ using isolated tumor specimens. All animals showing obvious tumors or morbidity were sacrificed for necropsy and histopathologic analyses. The animal experiments were approved by the Animal Ethical Committee and conducted in compliance with Centro de Investigaciones Energéticas, Medioambientales y Tecnológicas (CIEMAT) Guidelines.

Histologic and immunohistochemical procedures. Samples were fixed in 4% buffered formalin or in 70% ethanol and embedded in paraffin wax. Sections (5 μm) were stained with H&E or processed for immunohistochemistry. Mice were injected i.p. with bromodeoxyuridine (BrdUrd; 0.1 mg/g weight in 0.9% NaCl; Roche) 1 h before sacrifice. Immunohistochemistry and immunofluorescence were done using standard protocols on deparaffinized sections using antibodies against K5, K6 (1:500; Covance), K10 (k8.60, 1:500; Sigma), K17 (kindly provided by Dr. P. Coulombe, The Johns Hopkins University School of Medicine, Baltimore, MD), and K15 (1:50; NeoMarkers). BrdUrd incorporation was monitored by double immunofluorescence in ethanol-fixed samples or in formalin-fixed sections using an anti-BrdUrd antibody (1:50; Roche) as described in the manufacturer's instructions. For detection of active Akt (phosphorylated Akt Ser^{473}; 1:500; Cell Signaling), phosphorylated extracellular signal-regulated kinase (ERK; 1:500; Santa Cruz Biotechnology), cyclin D1 (ready to use; Lab Vision, NeoMarkers), and Foxo3a (1:500; Upstate), the slides were microwaved for 15 min. Immunodetection of CD31 (1:50; PharMingen) and α-smooth muscle actin (αSma; 1:200; Sigma) in endothelial cells was performed in frozen tumor sections fixed in cold acetone (5 min). Microvessel density, counting, and maturation were analyzed as previously described (24). Biotin-conjugated, FITC-conjugated, and Texas red–conjugated secondary antibodies were purchased from Jackson ImmunoResearch Laboratories and used at 1:1,000, 1:50, and 1:500, respectively. Apoptosis was detected with a double immunofluorescence using anti-K5 (to detect epidermal cells) and terminal deoxynucleotidyl transferase–mediated dUTP nick end labeling (*In situ* Cell Death Detection kit, Roche) according to the manufacturer's recommendations. Peroxidase was visualized using avidin-biotin complex method and 3,3′-diaminobenzidine kit (Vector). Control slides were obtained by replacing the primary antibodies with PBS (data not shown).

Western blot analysis. Whole skin extracts were ground with a mortar on liquid nitrogen and homogenized in buffer P [Tris (pH 7.5), 150 mmol/L NaCl, 1 mmol/L EDTA, 1 mmol/L EGTA, 40 mmol/L β-glycerophosphate, 1 mmol/L sodium orthovanadate, 0.1 mmol/L phenylmethylsulfonyl fluoride, 2 mg/mL aprotinin, 2 mg/mL leupeptin, 1% NP40]. Total protein (35 μg) from at least three pooled samples was used for NuPAGE 4% to 12% Bis-Tris gel (Invitrogen), transferred to nitrocellulose membrane (Invitrogen), and probed with primary antibodies against Akt, ERK2, phosphorylated ERK1/2, EGFR, phosphorylated tyrosine, Sprouty 2, Errfi1 (Santa Cruz Biotechnology), and phosphorylated Akt (Cell Signaling). Actin (Santa Cruz Biotechnology) was used to normalize the loading. Secondary antibodies anti-rabbit, anti-mouse, or anti-goat IgG were purchased from Jackson ImmunoResearch Laboratories. Chemiluminescence was performed using the manufacturer's recommendations (Pierce).

RNA purification and Affymetrix mouse GeneChip 430A analysis. Newborn mouse skin tissue was preserved in RNAlater (Ambion) and disrupted and homogenized using Mixer Mill MM301 (Retsch). Total RNA was extracted and purified from 30 mg of skin using RNeasy Fibrous Tissue Mini kit (Qiagen) following the manufacturers' recommendations. The integrity of the RNA populations was tested in the Bioanalyzer (Agilent) showing at least 1.4 28S to 18S ratio. Hybridization of pooled samples from three animals of each genotype into Affymetrix MOE 430A microarrays was performed per duplicate at the Genomic Facility of the Cancer Research Center (Salamanca, Spain). We exported CEL files from Affymetrix GeneChip Operating Software and performed background substraction with robust multichip average (25) and normalized the chips with the quantile method (26) using the Gene Expression Pattern Analysis Suite (27). The signal intensity values of each probe set were $\log_2$ transformed. Further analyses were performed using the MeV software (28). The selection of genes differentially expressed between control and mutant mice (1,435 gene IDs) was made using ANOVA analysis ($P \leq 0.01$). The list of significant genes implicated in phosphatidylinositol 3-kinase/Akt pathway and angiogenesis process was searched using Gene Ontology Biological Process.

Results

Phenotypic consequences of *Rb* and *Trp53* ablation in epidermis. The epidermis from mice lacking *Trp53* ($Rb^{wt/wt}$;$Trp53^{F2/F10}$;K14*cre*, thereafter $pRb^{+/+}$;$p53^{-/-}$) was normal and indistinguishable from wild-type mice (Fig. 1*A*). In contrast, *Rb* depletion in epidermis ($Rb^{F19/F19}$;$Trp53^{wt/wt}$;K14*cre*, thereafter $pRb^{-/-}$;$p53^{+/+}$) leads to moderate hyperplasia, which is not further increased by *Trp53* loss in double-deficient mice ($Rb^{F19/F19}$;$Trp53^{F2/F10}$;K14*cre*, thereafter $pRb^{-/-}$;$p53^{-/-}$; Fig. 1*A*). Differentiation analysis (Fig. 1*B*) revealed no abnormalities in the expression of various keratins (K5, K6, K10, K17, and K15) or other differentiation proteins (filaggrin, loricrin, and involucrin) in mice bearing the epidermal-specific ablation of *Trp53* compared with control mice (Fig. 1*B*; data not shown). As reported (17), pRb-deficient epidermis displayed expansion of K5 into suprabasal layers, coexpression of K5 and K10, and induction of K6 in some areas of the interfollicular epidermis. Again, these alterations are not further aggravated by subsequent loss of *Trp53* (Fig. 1*B*; data not shown).

Epidermal proliferation, analyzed by BrdUrd incorporation, showed no significant increase in the *Trp53*-deficient epidermis compared with wild-type epidermis (Supplementary Fig. S1; see also Fig. 4*A*). In agreement with our previous data (17), we found increased proliferation in pRb-deficient epidermis, which was nonaugmented by the simultaneous absence of both tumor suppressors in the interfollicular epidermis. Interestingly, we observed increased proliferation in hair follicles of $pRb^{-/-}$;$p53^{-/-}$ mice (see below). Finally, we also observed a significant BrdUrd incorporation in some scattered dermal cells in the dermis (denoted by *arrows* in Supplementary Fig. S1) in $pRb^{+/+}$;$p53^{-/-}$ and $pRb^{-/-}$;$p53^{-/-}$ samples.

Collectively, these observations show that the epidermal-specific ablation of p53 does not produce any obvious phenotypic abnormalities nor aggravate those produced by pRb ablation with respect to proliferation and differentiation, being the only alteration detected the abnormal proliferation of scattered cells in the dermis.

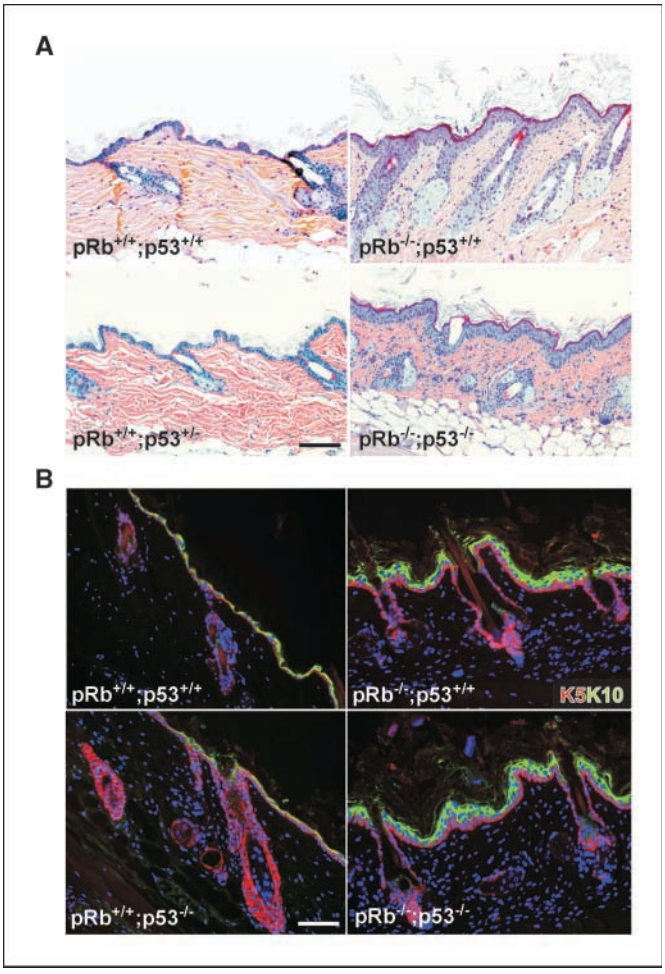

Figure 1. Phenotypic consequences of *Rb* and *Trp53* ablation in epidermis. *A,* H&E-stained skin sections of pRb$^{+/+}$;p53$^{+/+}$ (*Rb*$^{wt/wt}$;*Trp53*$^{wt/wt}$;K14*cre*), pRb$^{-/-}$;p53$^{+/+}$ (*Rb*$^{F19/F19}$;*Trp53*$^{wt/wt}$;K14*cre*), pRb$^{+/+}$;p53$^{-/-}$ (*Rb*$^{wt/wt}$;*Trp53*$^{F2/F10}$;K14*cre*), and pRb$^{-/-}$;p53$^{-/-}$ (*Rb*$^{F19/F19}$;*Trp53*$^{F2/F10}$;K14*cre*) adult mice showing a moderate hyperplasia with pRb loss, which is not aggravated by the simultaneous loss of pRb and p53. *B,* immunofluorescence analysis showing the expression of the keratin K5 (*red*) and differentiation keratin K10 (*green*) in the epidermis of the control and the quoted mutant mice. pRb absence induces an expansion of K5 into suprabasal layers and a coexpression of K5 and K10. These alterations are not aggravated by p53 loss. *Bar,* 100 μm.

Spontaneous tumors in mice bearing the *Rb* and *Trp53* ablation in epidermis. Despite the fact that p53 loss in epidermis did not cause any evident phenotype in nonlesional skin, we observed that all the mice lacking p53 in epidermis developed spontaneous tumors (Fig. 2*A*). The onset of appearance of these lesions is 5 months of age and all the mice developed tumors by 12 months of age (median, 8.3 ± 1.1 months). The tumor susceptibility is accelerated in double-deficient mice (Fig. 2*A*), where we observed that the onset of tumor appearance was 3 months and all mice developed tumors by 8 months (median, 5.5 ± 1.4 months; $P \leq 0.0009$). The multiplicity of tumors is also increased in double-deficient mice compared with *Trp53*-deficient mice (3.4 ± 0.7 versus 1.1 ± 0.8, respectively; $P \leq 0.0006$). Of note, the type and localization of the tumors were similar between pRb$^{+/+}$;p53$^{-/-}$ and pRb$^{-/-}$;p53$^{-/-}$ mice and almost exclusively affected different areas of the skin, such as neck, snout, perianal, face, and back skin, which in most cases do not produce external wounds. Histology analysis revealed that all these tumors were predominantly epidermal SCCs (84.5% of 197 tumors analyzed). These results showed that p53 is an essential tumor suppressor in epidermis, in agreement with others (21, 22, 29). In addition, our data also indicate that pRb and p53 cooperate to suppress mouse skin tumorigenesis.

To further analyze the cooperation between both tumor suppressors, we performed a detailed study of tumor development in a large cohort of mice bearing different combinations of *Trp53* and *Rb* alleles. In these analyses, we found that *Rb* heterozygosity did not increase the rate of appearance of tumors in mice lacking *Trp53* (Fig. 2*B*). On the other hand, *Trp53* heterozygosity in pRb$^{-/-}$ mice leads to spontaneous tumor development, although it is significantly delayed compared with complete *Trp53* loss (Fig. 2*C*). We also detected loss of the remaining *Trp53* allele in some tumors of pRb$^{+/-}$;p53$^{+/-}$ and pRb$^{-/-}$;p53$^{+/-}$ mice (data not shown). The rate of appearance of tumors was similar between pRb$^{+/-}$;p53$^{+/-}$ and pRb$^{-/-}$;p53$^{+/-}$ (Fig. 2*C*). Consequently, the tumor susceptibility attributable to *Trp53* loss, either complete or in heterozygosis, is only accelerated by the complete loss of *Rb*.

Hair follicle origin of spontaneous tumors. The vast majority of the tumors observed in all the genotypes correspond to poorly differentiated SCCs with loss or reduced expression of suprabasal keratins K10, K6, and K17 (Fig. 3*A*). Interestingly, the study of skin of tumor-bearing mice revealed multiple dysplastic hair follicles, which in most cases are also characterized by the presence of tumoral cell masses arising from the tip of these structures (Fig. 3*B*). This suggests that the tumors might have a hair follicle origin. This observation was further supported by the finding that early-stage tumors, associated with dysplastic hair follicles, express markers such as keratins K15 and K17 in addition to the basal keratin K5 (Fig. 3*B*) and suprabasal K6 (data not shown). Importantly, the incidence of these type of lesions is higher in pRb$^{-/-}$;p53$^{-/-}$ (41.6%; n = 36) compared with pRb$^{+/+}$;p53$^{-/-}$ (23.5%; n = 17) mice.

The augmented proliferation observed in pRb$^{-/-}$;p53$^{-/-}$, compared with pRb$^{+/+}$;p53$^{-/-}$ mouse epidermis and hair follicles (Supplementary Fig. S1), would suggest that this process could be involved in the increased tumor susceptibility observed in pRb$^{-/-}$;p53$^{-/-}$ mice. We have thus monitored BrdUrd incorporation in nonlesional interfollicular epidermis, nonlesional and dysplastic hair follicles, and tumors at early and advanced stage (Fig. 4*A*; Supplementary Figs. S1 and S2). We observed a significant increase in proliferation in pRb$^{-/-}$;p53$^{-/-}$ nonlesional hair follicles, which was similar to that displayed by dysplastic hair follicles and early-stage and advanced tumors (Fig. 4*A*). Notably, the pRb$^{+/+}$;p53$^{-/-}$ nonlesional hair follicles did not show such increased proliferation (Fig. 4*A*; see also Supplementary Fig. S1). A moderate increase in BrdUrd incorporation was only observed in p53-deficient early lesions (Fig. 4*A*; see also Supplementary Figs. S1 and S2) but below the proliferation rate of advanced tumors (Fig. 4*A*). However, we did not detect significant changes in proliferation between pRb$^{+/+}$;p53$^{-/-}$ and pRb$^{-/-}$;p53$^{-/-}$ tumors at advanced stage (Fig. 4*A*) probably because the pRb$^{+/+}$;p53$^{-/-}$ tumors have selected for loss of *Rb* function.

We next studied possible differences in apoptosis. In agreement with the key roles of p53 modulating this process, the apoptotic rate was extremely low in all the cases. Moreover, we did not detect significant differences in the apoptotic rate between pRb$^{+/+}$;p53$^{-/-}$ and pRb$^{-/-}$;p53$^{-/-}$ mice in normal or dysplastic hair follicles nor in tumors either at early or advanced stage (data not shown; Supplementary Fig. S3).

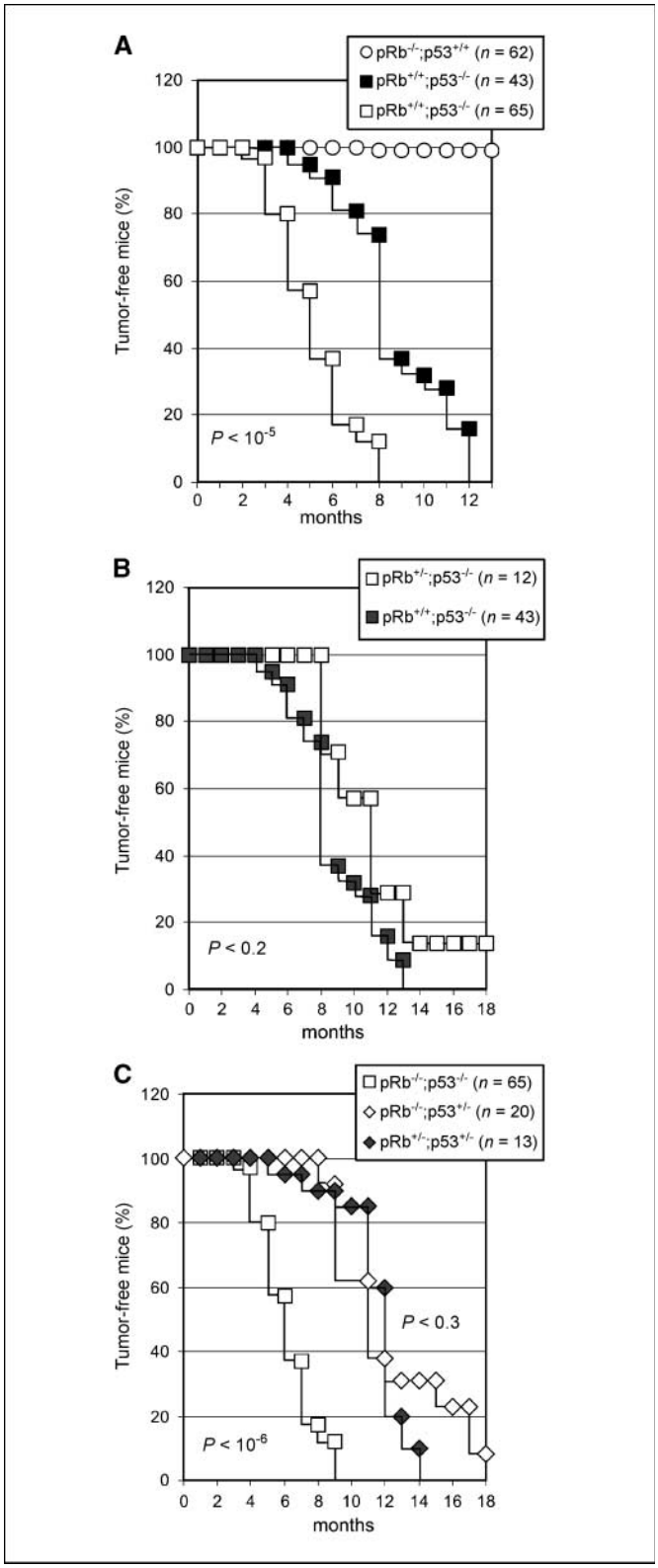

Figure 2. Spontaneous tumorigenesis in mice bearing the *Rb* and *Trp53* ablation in epidermis. Kaplan-Meier distribution of tumor-free mice as a function of age (months) comparing pRb$^{-/-}$;p53$^{-/-}$ (*Rb*$^{F19/F19}$;*Trp53*$^{F2/F10}$;K14*cre*; $n = 65$), pRb$^{+/+}$;p53$^{-/-}$ (*Rb*$^{wt/wt}$;*Trp53*$^{F2/F10}$;K14*cre*; $n = 43$), and pRb$^{-/-}$;p53$^{+/+}$ (*Rb*$^{F19/F19}$;*Trp53*$^{wt/wt}$;K14*cre*; $n = 62$; *A*); pRb$^{+/-}$;p53$^{-/-}$ ($n = 12$) and pRb$^{+/+}$;p53$^{-/-}$ ($n = 43$; *B*); and pRb$^{-/-}$;p53$^{-/-}$ ($n = 65$), pRb$^{+/-}$;p53$^{+/-}$ ($n = 13$), and pRb$^{-/-}$;p53$^{+/-}$ ($n = 20$; *C*). *n,* number of mice of each genotype analyzed. The values of *P* for paired samples are provided.

Collectively, these data indicate that the increased incidence and early appearance of tumors in pRb$^{-/-}$;p53$^{-/-}$ mice is attributable to increased proliferation but not to altered apoptosis in hair follicles, leading to early dysplasia and malignant conversion.

We also monitored the growth rate of the tumors. However, as the dysplastic and early-stage tumors were only detectable during histology analyses, we focused only in advanced isolated tumors. We observed increased volume in double-deficient mice tumors compared with p53-deficient tumors in age-matched samples (Fig. 4*B*). This result indicates that, in spite of similar proliferation rates, double-deficient tumors might have alternative mechanisms leading to augmented tumor growth.

Finally, as the SCC can undergo epithelial mesenchymal transition (EMT) leading to the formation of highly aggressive spindle cell carcinomas, we analyzed whether EMT is increased in the absence of pRb and p53. A significant number of spindle cell carcinomas was observed in pRb$^{+/+}$;p53$^{-/-}$ and pRb$^{-/-}$;p53$^{-/-}$ mice (Supplementary Fig. S4). We found that the rate of appearance of spindle cell carcinomas is slightly accelerated in pRb$^{-/-}$;p53$^{-/-}$ compared with pRb$^{+/+}$;p53$^{-/-}$ (Supplementary Fig. S4). However, the rate of conversion of SCC into spindle cell carcinoma was similar between the two genotypes (Supplementary Fig. S4), suggesting that EMT is not significantly altered in double-deficient tumors.

Molecular mechanisms of cooperative functions between pRb and p53. The cooperation between pRb and p53 has not been previously described in epidermal tumorigenesis. To characterize the molecular basis that may justify the accelerated tumor development in doubly deficient mice, we focused on the possible involvement of specific signal transduction pathways. The Akt and mitogen-activated protein kinase (MAPK)/ERK signaling pathways have been shown as key processes in mouse skin tumorigenesis (30, 31). Therefore, we analyzed the activation of these pathways in the spontaneous tumors (Fig. 5*A*). Compared with pRb$^{+/+}$;p53$^{-/-}$, pRb$^{-/-}$;p53$^{-/-}$ tumors displayed increased phosphorylation of Akt (Fig. 5*A*). Similarly, pRb$^{-/-}$;p53$^{-/-}$ tumors displayed increased ERK1/2 phosphorylation compared with tumors arising in pRb$^{+/+}$;p53$^{-/-}$ mice (Fig. 5*A*). However, in this case, phosphorylated ERK was mainly localized in the tumor stroma rather than in tumoral cells. In agreement with the increased Akt activation, we observed that pRb$^{-/-}$;p53$^{-/-}$ tumors displayed increased nuclear localization of cyclin D1, whereas Foxo3a showed almost exclusively cytoplasmic localization compared with tumors from pRb$^{+/+}$;p53$^{-/-}$ mice (Fig. 5*A*). Because the increase in Akt activity would justify the increase in proliferation observed in pRb$^{-/-}$;p53$^{-/-}$ hair follicles, which precedes tumor development, we analyzed whether the activation of Akt takes place in nonlesional epidermis. Western blot showed increased phosphorylated Akt and decreased phosphorylated ERK2 in pRb$^{-/-}$;p53$^{-/-}$ nonlesional skin (Fig. 5*B*). Moreover, microarray analyses showed that multiple genes involved in EGFR/Akt/ERK pathway were deregulated in pRb$^{-/-}$;p53$^{-/-}$ newborn skin (Fig. 5*C*). In particular, we found decreased expression of *Errfi1*, which acts as a negative regulator of EGFR signaling, whereas some ligands, such as *Btc*, are up-regulated. We confirmed by Western blot the increased tyrosine phosphorylation and thus activation of EGFR in skin of double-deficient mice without increased EGFR expression and in parallel with decreased Errfi1 expression (Fig. 5*B*). These data may justify the increased Akt activity observed in nonlesional skin. This activation is also supported by the increased expression of *Igf2, Pdgfa*, and *Pdpk1* genes (Fig. 5*C*). In addition, we also observed increased expression

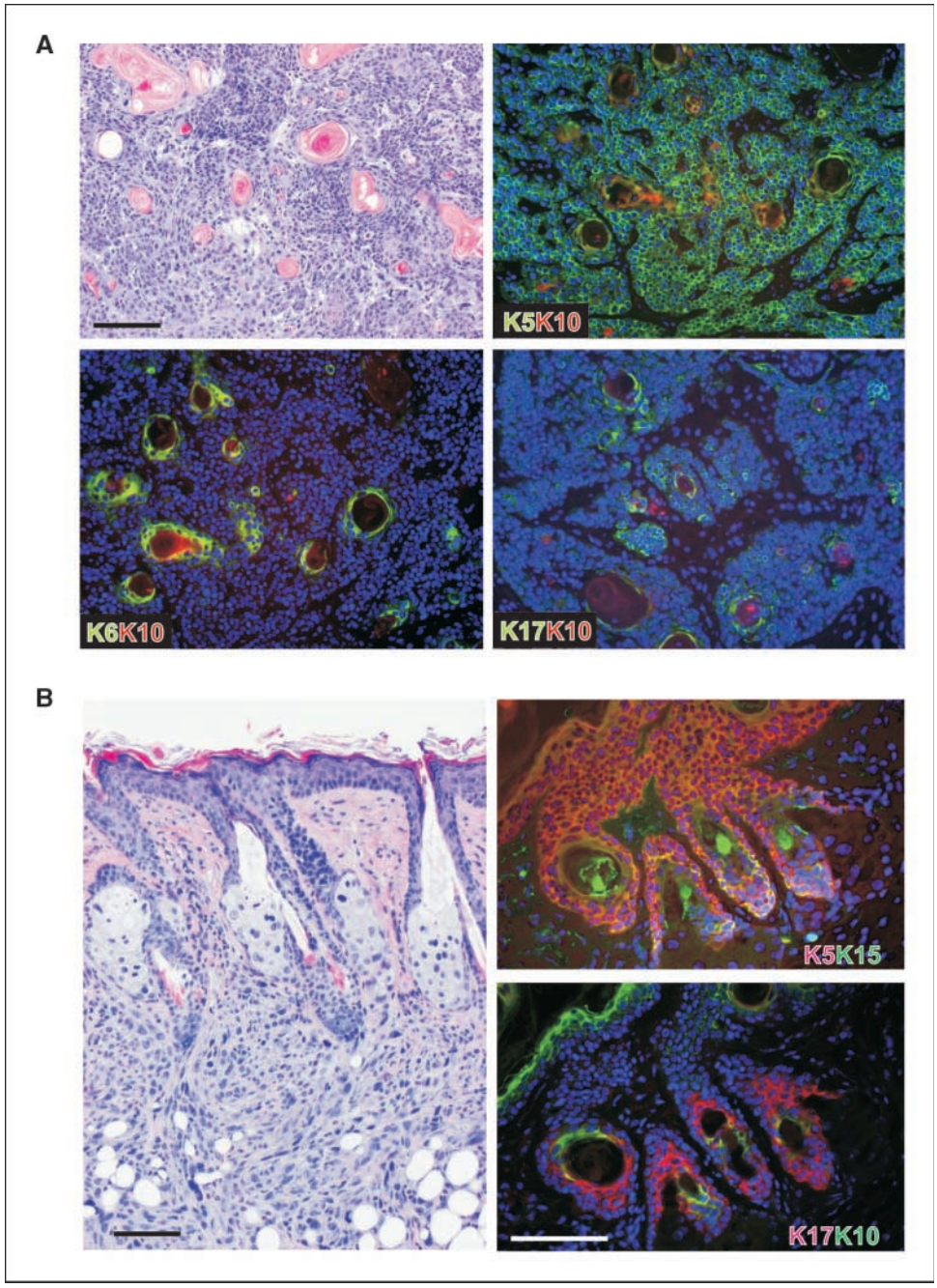

Figure 3. Hair follicle origin of spontaneous tumors. *A,* histology and immunofluorescence analysis of poorly differentiated SCCs from a $pRb^{-/-}$;$p53^{-/-}$ (*Rb*$^{F19/F19}$;*Trp53F2*$^{/F10}$;K14*cre*) mouse showing the sustained expression of K5 and reduced expression of K10, K6, and K17 (colors in tabs denote the specific keratin). *B,* H&E-stained section showing a representative example of s.c. tumor mass arising from the hair follicle in a $pRb^{-/-}$;$p53^{-/-}$ (*Rb*$^{F19/F19}$;*Trp53*$^{F2/F10}$;K14*cre*) mouse. The expression of K5 (*red*) and K15 (*green*) and K17 (*red*) and K10 (*green*) supports the possible follicular origin of these lesions. *Bar,* 100 μm.

of *Spry2* (Fig. 5*C*), whose gene product, Sprouty 2, inhibits the activation of MAPK pathway induced by activated EGFR (32). We observed increased expression of Sprouty 2 in the skin of mice lacking p53, which was more evident in $pRb^{-/-}$;$p53^{-/-}$ skin (Fig. 5*B*). This finding may help to explain why the activation of EGFR leads to increased Akt, but not ERK activity, in the pretumoral stages of $pRb^{-/-}$;$p53^{-/-}$ skin.

The absence of *Rb* and *Trp53* induces a premature increased angiogenic response. The increased Akt activity found in tumors and pretumoral skin would be responsible for the increased susceptibility to spontaneous tumor development. Akt signaling is involved in increased proliferation and decreased apoptosis (33–35). Moreover, we have recently observed that the expression of a constitutively active Akt in mouse epidermis leads to spontaneous tumor formation and heightened susceptibility to chemical carcinogenesis mainly through the increase in proliferative signals (36). This may be responsible for the accelerated appearance of tumors in $pRb^{-/-}$;$p53^{-/-}$ skin. However, we did not observe alterations in proliferation or apoptosis in advanced tumors lacking *Rb* and *Trp53* compared with those observed in mice lacking *Trp53* (Fig. 4*A*; Supplementary Figs. S2 and S3), whereas a significant increase in growth was observed in $pRb^{-/-}$;$p53^{-/-}$ tumors (Fig. 4*B*), indicating that other processes can be involved. There is broad evidence on the involvement of PTEN/Akt signaling in tumor angiogenesis (37, 38), and we have observed that Akt may specifically mediate an angiogenic switch in keratinocytes through transcriptional and posttranscriptional mechanisms (24, 39). In support of this, the appearance of $pRb^{-/-}$;$p53^{-/-}$ tumors suggests

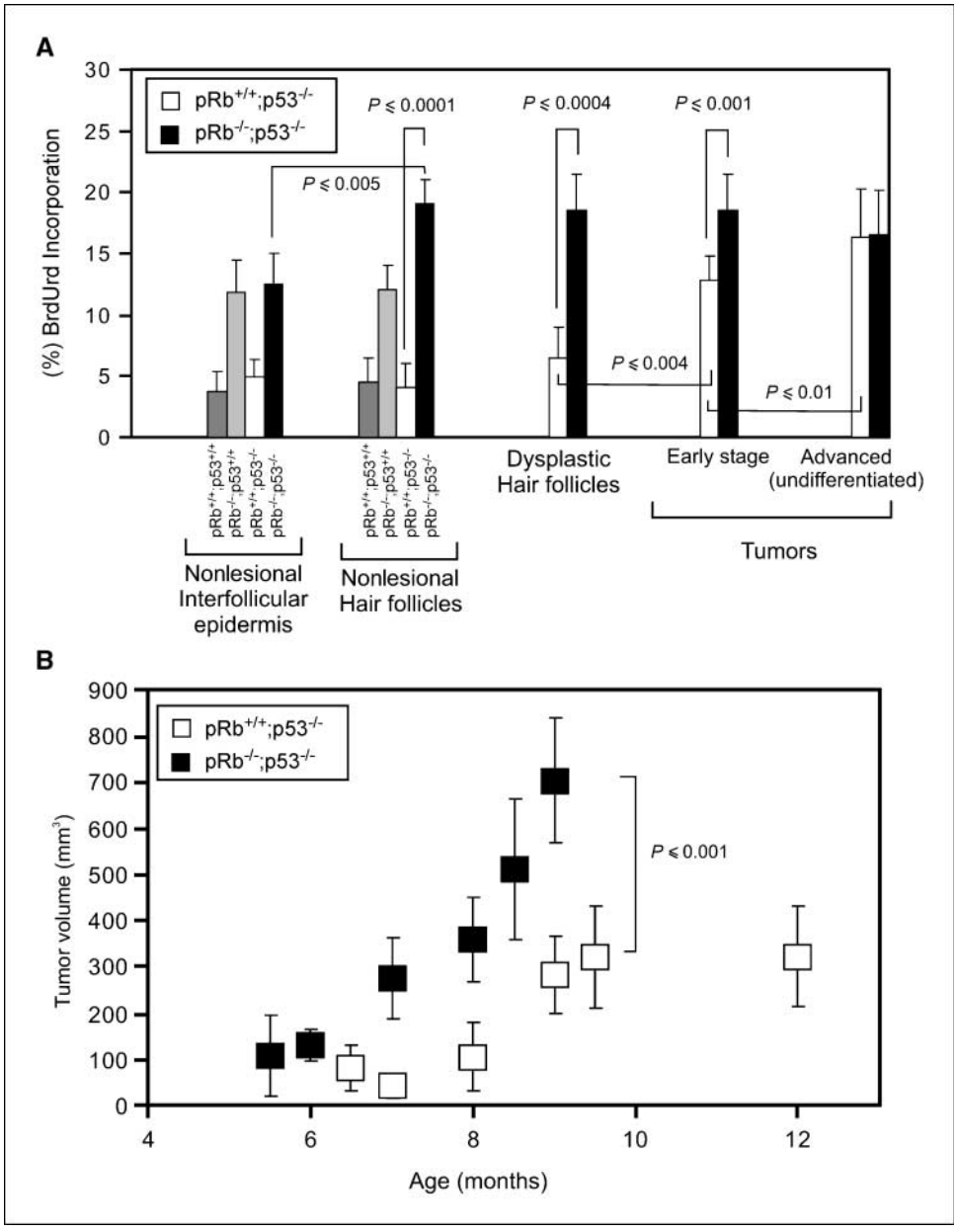

Figure 4. Proliferation and growth in spontaneous tumors. *A,* percentage of BrdUrd incorporation in interfollicular epidermis, nonlesional and dysplastic hair follicles, and tumors at early or advanced stage. Data come from the analysis of at least 10 different samples. *Columns,* mean; *bars,* SE. *B,* median volume (±SE) of the tumors isolated from $pRb^{-/-};p53^{-/-}$ (*Rb*$^{F19/F19}$;*Trp53*$^{F2/F10}$; K14*cre*) and $pRb^{+/+};p53^{-/-}$ (*Rb*$^{wt/wt}$; *Trp53*$^{F2/F10}$;K14*cre*) at different ages (months). The values of *P* obtained after *t* test of paired samples are provided.

increased vascularity (data not shown). Consequently, we monitored the possible changes in angiogenesis in tumors.

We analyzed the tumor-associated vascularization in frozen sections of the tumors, which were stained for the endothelial junction molecule CD31 (40). In $pRb^{+/+};p53^{-/-}$ and $pRb^{-/-};p53^{-/-}$ tumor samples (Fig. 6*A*), the vessels seemed similar to those observed in poorly differentiated carcinomas (40). However, an increased number of vessels were observed in doubly deficient tumors. To verify this observation in a quantitative manner, computer-assisted morphometric image analysis was performed in the CD31-stained sections. This revealed that both vessel density and the relative area occupied by tumor blood vessels were increased in $pRb^{-/-};p53^{-/-}$ tumors compared with $pRb^{+/+};p53^{-/-}$ samples (Fig. 6*B*). In support of this augmented angiogenic switch, we also detected that the number of mature vessels, coexpressing CD31 and the pericyte marker αSma (Fig. 6*A*), was reduced in double-deficient tumors compared with $pRb^{+/+};p53^{-/-}$ samples (Fig. 6*B*). Finally, the altered angiogenesis was further supported by microarray analysis, which also showed increased expression of multiple angiogenic factors, such as *Pdgfa, Pitx2*, and *Ptgs2* (cyclooxygenase 2), and decreased expression of antiangiogenic molecules, such as *Foxo1, Col18a1* (endostatin), and *Timp3*, in double-deficient newborn skin (Fig. 6*C*).

Collectively, these results indicate that the increased growth of $pRb^{-/-};p53^{-/-}$ tumors is also supported by increased angiogenesis.

Discussion

SCCs are, together with BCC, the prevalent tumor types of NMSC (2). SCCs are characterized by increased aggressiveness and metastatic properties, but the molecular basis of their development is still poorly understood. This is a relevant issue as the immunosuppressed population of organ-transplanted patients displays severely increased susceptibility to SCC occurrence (2), mediated

in part by cutaneous HPV infection. The relevance of SCC in human tumorigenesis is also highlighted because it is the most frequent type of tumor in head and neck and cervix and also occurs as a minor metaplastic type in breast and lung. All these aspects reinforce the necessity of developing more accurate models of SCC that can be used as preclinical tools.

The tumorigenic properties of HPV have been associated with the expression of E6 and E7 oncoproteins, which target the p53- and the pRb-dependent pathways, respectively (2). This has led us to hypothesize that the ablation of *p53* and *pRb* genes would recapitulate SCCs. Previous work has shown that the specific ablation of *p53* gene in stratified epithelia confers high susceptibility to skin SCC development (21, 22, 29). Our present data agree with these observations. On the contrary, the epidermal-specific ablation of *Rb* gene does not confer susceptibility to spontaneous skin tumor development (17), and on chemical carcinogenesis experiments, the absence of pRb in epidermis produced increased resistance to tumorigenesis but also higher malignant rate of conversion (19). These aspects have been previously associated to the induction of p53, which causes a selective pressure leading to the premature loss of p53 functions (19, 20). In support of these findings, we have also observed that the simultaneous absence of pRb and p107 leads to spontaneous tumor formation in part through the abrogation of p53-dependent apoptotic processes (18).[1] These data suggest that the simultaneous absence of p53 and pRb would cooperate in the skin tumor

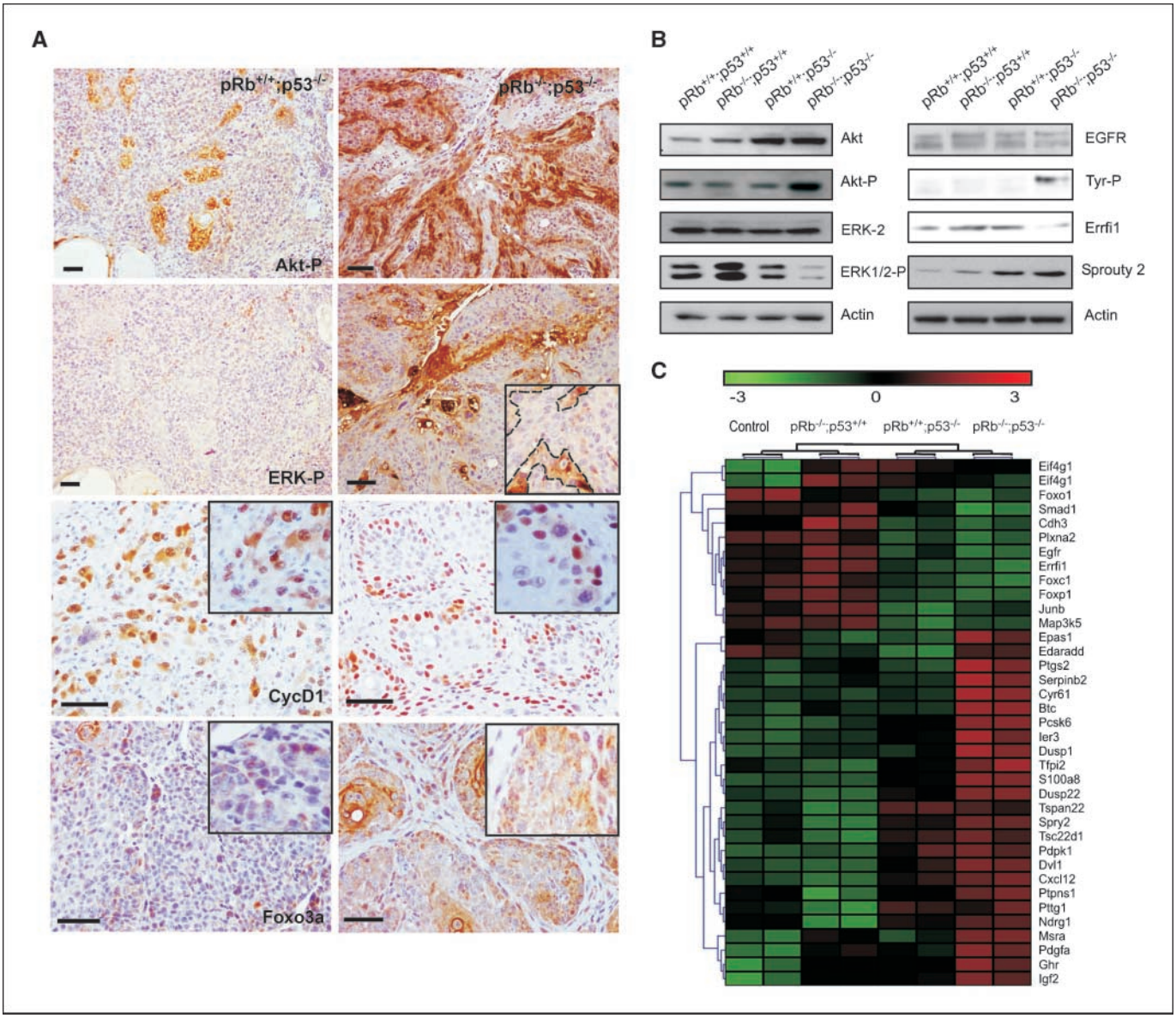

Figure 5. Activation studies of Akt and MAPK/ERK signaling pathways in pRb$^{+/+}$;p53$^{-/-}$ and pRb$^{-/-}$;p53$^{-/-}$ spontaneous tumors. *A,* immunohistochemical detection of phosphorylated Akt (*Akt-P*), phosphorylated ERK (*ERK-P*), cyclin D1 (*CycD1*), and Foxo3a in pRb$^{+/+}$;p53$^{-/-}$ (*Rb*$^{wt/wt}$;*Trp53*$^{F2/F10}$;K14*cre*) and pRb$^{-/-}$;p53$^{-/-}$ (*Rb*$^{F19/F19}$;*Trp53*$^{F2/F10}$;K14*cre*) spontaneous tumors. *Insets,* higher magnification of representative fields. *Bar,* 150 μm. *B,* biochemical analysis of pooled whole nonlesional skin extracts obtained from mice of the quoted genotypes used to examine the status of Akt, ERK2, EGFR, Errfi1, and Sprouty 2. Actin was used as a loading control. *C,* heat map graphical representation showing the relative expression of MAPK and Akt pathway-related gene IDs after microarray analysis of newborn skin of mice of the quoted genotypes.

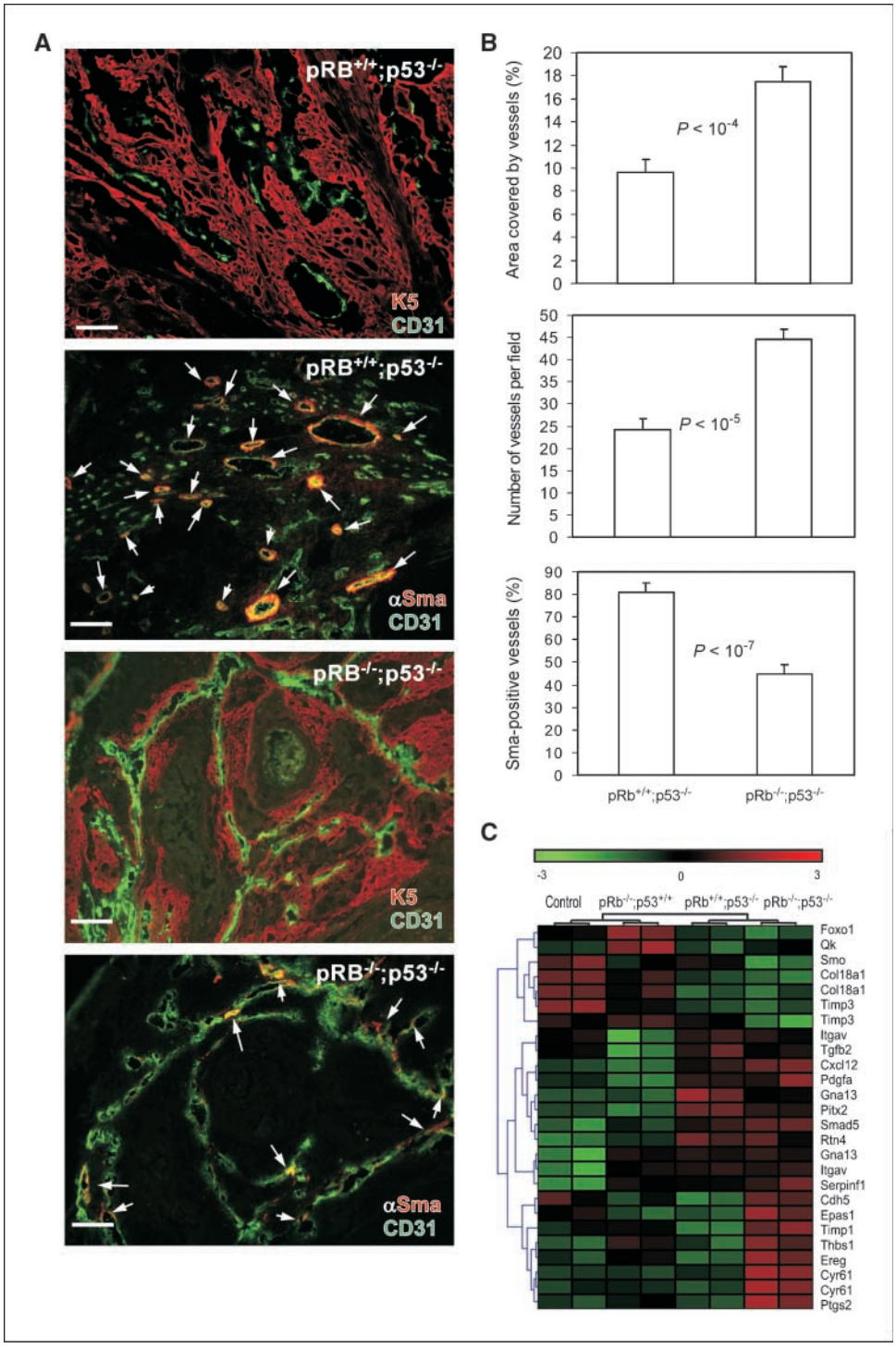

Figure 6. Angiogenic response in pRb$^{+/+}$;p53$^{-/-}$ and pRb$^{-/-}$;p53$^{-/-}$ spontaneous tumors. *A,* examples of the immunofluorescence analysis of epithelial keratin K5, endothelial junction molecule CD31, and pericyte marker αSma in pRb$^{+/+}$;p53$^{-/-}$ (*Rb*$^{wt/wt}$;*Trp53*$^{F2/F10}$;K14*cre*) and pRb$^{-/-}$;p53$^{-/-}$ (*Rb*$^{F19/F19}$;*Trp53*$^{F2/F10}$;K14*cre*) spontaneous tumors. *Bar,* 100 μm. *B,* quantitative analysis of the percentage of area covered by blood vessels, number of blood vessels per field, and percentage of αSma-positive vessels in spontaneous tumors showing the increased vascularization in pRb$^{-/-}$;p53$^{-/-}$ (*Rb*$^{wt/wt}$;*Trp53*$^{F2/F10}$;K14*cre*) compared with pRb$^{+/+}$;p53$^{-/-}$ (*Rb*$^{F19/F19}$;*Trp53*$^{F2/F10}$;K14*cre*). Data come from five to nine different tumors of each genotype. *Columns,* mean; *bars,* SE. The values of *P* for paired samples are provided. *C,* heat map graphical representation showing the relative expression of genes involved in angiogenic processes obtained after microarray analysis of newborn skin of mice of the quoted genotypes.

formation as previously reported for prostate, lung, and cerebellum tumors (14–16).

The present data, besides confirming the relevance of p53 as a tumor suppressor in epidermis (41), also show that the simultaneous absence of pRb and p53 accelerates the rate of tumor appearance. The importance of p53 in suppressing mouse tumor development has been previously shown in multiple tissues, including epidermis (42, 43). In this last case, it has been shown that depletion of *p53* gene, or generation of epidermal-specific knock in, produces spontaneous tumors and increases the susceptibility to carcinogenic treatments (21, 22, 29). Therefore, we have studied in depth the mechanisms that might confer the increased susceptibility in the absence of *Rb* and *Trp53*.

We found that the loss of p53 in epidermis has no significant consequences in terms of proliferation and/or differentiation nor it aggravates these alterations caused by specific *Rb* loss. Nonetheless, we observed augmented proliferation in pRb$^{-/-}$;p53$^{-/-}$ pretumoral hair follicles, which might be responsible for

the observed increased tumor development. Indeed, the tumors were initially detected as s.c. masses, and histology revealed pretumoral alterations in hair follicle structures. It is worth mentioning that the putative epidermal stem cells are located in these structures (44), which could indicate that the absence of these tumor suppressors might have a functional effect on this cell population. A similar observation has been recently shown in the prostate in close relationship with carcinogenesis (45). In support of this suggestion, we found an increased number of cells expressing K15, a putative marker of epidermal stem cells (46) in the early lesions. However, we did not find K15-positive cells in advanced tumors. This may indicate that the K15-positive cells either are lost or change their phenotypic characteristics during tumor progression.

On the other hand, we did not find significant apoptosis in skin or differences in apoptotic rates between $pRb^{+/+};p53^{-/-}$ and $pRb^{-/-};p53^{-/-}$ tumors. This is in contrast with the increased apoptosis observed in the tumors generated by chemical carcinogenesis in pRb-deficient mice (19) and reinforces the previous suggestion that, on oncogenic stress, the absence of pRb can cause apoptosis in a p53-dependent manner (20).[1]

The Akt and MAPK signaling pathways have been previously involved in the genesis of SCC in mouse skin (30, 36, 39). We thus investigated whether these pathways act differentially in $pRb^{+/+};p53^{-/-}$ and $pRb^{-/-};p53^{-/-}$ tumors. The data clearly showed an increased Akt activity leading to increased nuclear cyclin D1 and cytoplasmic Foxo3a localization in $pRb^{-/-};p53^{-/-}$ tumors. These data are in close parallelism with the findings obtained in human head and neck SCC and Akt-transformed mouse keratinocytes (39, 47). On the other hand, the apparent increase in MAPK was significantly confined to the stromal component of the $pRb^{-/-};p53^{-/-}$ tumors. This would imply that this signaling pathway is not responsible for the increased tumorigenicity, at least in a cell autonomous process, and suggests that several changes occur in the stroma of these tumors. Whether these changes may affect the tumor development remains unknown at present. The absence of active ERK1/2 in nonlesional mouse skin extracts, in contrast with the increased Akt activity, supports the hypothesis that MAPK signaling contributes to the maintenance but not to the generation of the tumors. Notably, such increase in Akt activity seems to be mediated by increased EGFR signaling. This pathway has a dramatic relevance in SCC in human and mice. Our data indicate that, in $p53^{-/-};pRb^{-/-}$ skin, this increased signaling does not proceed through increased EGFR expression but rather down-regulation of negative regulators of this pathway, such as *Errfi1*. In this regard, it has been shown that the *Errfi1*$^{-/-}$ mice develop spontaneous tumors in various organs and are highly susceptible to chemically induced formation of skin tumors (48). EGFR activation can trigger both MAPK/ERK and Akt activity; however, in the absence of *Egfr* amplification, activating mutations of EGFR selectively activate Akt but have no effect on ERK signaling (49). Our data completely fit into this aspect. In addition, the ectopic Sprouty 2 expression observed in doubly deficient skin can contribute to this finding. This putative tumor suppressor can be induced by EGFR/MAPK signaling and produces the feedback inhibition of MAPK/ERK (50).

Akt activities in oncogenesis are diverse and have been mainly associated with the inhibition of apoptosis and increased proliferation (35, 37). However, as mentioned above, we did not detect decreased apoptosis or increased proliferation in $pRb^{-/-};p53^{-/-}$ compared with $pRb^{-/-};p53^{+/+}$ tumors at advanced stage. Moreover, in spite of these similar proliferation rates, there is increased tumor growth in $pRb^{-/-};p53^{-/-}$ mice, suggesting an alternative mechanism. In this regard, the PTEN/Akt pathway has also been involved in tumorigenesis through nonautonomous cell mechanisms that include angiogenic switch (37). In support of this, we found increased number of blood vessels, which also display immaturity features, in $pRb^{-/-};p53^{-/-}$ compared with $pRb^{+/+};p53^{-/-}$ tumors and altered expression of genes involved in angiogenesis. These observations agree with the reported increased angiogenesis in HPV16 E6- and E7-transduced human primary keratinocytes (51) and our previous data showing that increased Akt activity may mediate an increase in skin tumorigenesis through increased angiogenesis (24).

Collectively, we report the generation of a mouse model of SCC through the epidermal ablation of *Rb* and *Trp53* genes. We have also carried out a detailed molecular characterization of the signaling pathways responsible for the increased susceptibility of epidermal tumor development in this model. Functional comparative studies for the validation of the model as a preclinical tool are currently being performed. These will clearly open new possibilities of pharmacologic intervention for the treatment of these tumors.

Acknowledgments

Received 8/10/2007; revised 10/8/2007; accepted 11/12/2007.

Grant support: Oncocycle (CAM), ISCIII-RETIC RD06/0020 (MSC), SAF2005-00033 (MCYT), and Oncology Program from La Caixa Foundation (J.M. Paramio). M. Moral is a recipient of a FIS-BEFI Predoctoral Fellowship from MSC (BF03-00201).

The costs of publication of this article were defrayed in part by the payment of page charges. This article must therefore be hereby marked *advertisement* in accordance with 18 U.S.C. Section 1734 solely to indicate this fact.

We thank Dr. A. Berns (Netherlands Cancer Institute, Amsterdam, the Netherlands) for providing different mutant mice, Dr. P. Coulombe for the generous gift of anti-K17 antibody, Jesús Martínez and the personnel of the animal facility of CIEMAT for the excellent care of the animals, and Pilar Hernández (CIEMAT) for the histologic preparations.

References

1. Nickoloff BJ, Qin JZ, Chaturvedi V, Bacon P, Panella J, Denning MF. Life and death signaling pathways contributing to skin cancer. J Investig Dermatol Symp Proc 2002;7:27–35.
2. Boukamp P. Non-melanoma skin cancer: what drives tumor development and progression? Carcinogenesis 2005;26:1657–67.
3. Vogelstein B, Lane D, Levine AJ. Surfing the p53 network. Nature 2000;408:307–10.
4. Weinberg RA. The retinoblastoma protein and cell cycle control. Cell 1995;81:323–30.
5. Hickman ES, Moroni MC, Helin K. The role of p53 and pRB in apoptosis and cancer. Curr Opin Genet Dev 2002; 12:60–6.
6. Sherr CJ, McCormick F. The RB and p53 pathways in cancer. Cancer Cell 2002;2:103–12.
7. Brugarolas J, Bronson RT, Jacks T. p21 is a critical CDK2 regulator essential for proliferation control in Rb-deficient cells. J Cell Biol 1998;141:503–14.
8. Brugarolas J, Moberg K, Boyd SD, Taya Y, Jacks T, Lees JA. Inhibition of cyclin-dependent kinase 2 by p21 is necessary for retinoblastoma protein-mediated G_1 arrest after γ-irradiation. Proc Natl Acad Sci U S A 1999;96:1002–7.
9. Dimri GP, Nakanishi M, Desprez PY, Smith JR, Campisi J. Inhibition of E2F activity by the cyclin-dependent protein kinase inhibitor p21 in cells expressing or lacking a functional retinoblastoma protein. Mol Cell Biol 1996;16:2987–97.
10. DeGregori J, Leone G, Miron A, Jakoi L, Nevins JR. Distinct roles for E2F proteins in cell growth control and apoptosis. Proc Natl Acad Sci U S A 1997;94:7245–50.
11. Bates S, Phillips AC, Clark PA, et al. p14ARF links the tumour suppressors RB and p53. Nature 1998;395: 124–5.
12. Russell JL, Powers JT, Rounbehler RJ, Rogers PM, Conti CJ, Johnson DG. ARF differentially modulates

apoptosis induced by E2F1 and Myc. Mol Cell Biol 2002; 22:1360–8.
13. Tolbert D, Lu X, Yin C, Tantama M, Van Dyke T. p19(ARF) is dispensable for oncogenic stress-induced p53-mediated apoptosis and tumor suppression *in vivo*. Mol Cell Biol 2002;22:370–7.
14. Meuwissen R, Linn SC, Linnoila RI, Zevenhoven J, Mooi WJ, Berns A. Induction of small cell lung cancer by somatic inactivation of both Trp53 and Rb1 in a conditional mouse model. Cancer Cell 2003;4:181–9.
15. Shakhova O, Leung C, van Montfort E, Berns A, Marino S. Lack of Rb and p53 delays cerebellar development and predisposes to large cell anaplastic medulloblastoma through amplification of N-Myc and Ptch2. Cancer Res 2006;66:5190–200.
16. Zhou Z, Flesken-Nikitin A, Corney DC, et al. Synergy of p53 and Rb deficiency in a conditional mouse model for metastatic prostate cancer. Cancer Res 2006;66: 7889–98.
17. Ruiz S, Santos M, Segrelles C, et al. Unique and overlapping functions of pRb and p107 in the control of proliferation and differentiation in epidermis. Development 2004;131:2737–48.
18. Lara MF, Paramio JM. The Rb family connects with the Tp53 family in skin carcinogenesis. Mol Carcinog 2007;46:618–23.
19. Ruiz S, Santos M, Lara MF, Segrelles C, Ballestin C, Paramio JM. Unexpected roles for pRb in mouse skin carcinogenesis. Cancer Res 2005;65:9678–86.
20. Ruiz S, Santos M, Paramio JM. Is the loss of pRb essential for the mouse skin carcinogenesis? Cell Cycle 2006;5:625–9.
21. Derksen PW, Liu X, Saridin F, et al. Somatic inactivation of E-cadherin and p53 in mice leads to metastatic lobular mammary carcinoma through induction of anoikis resistance and angiogenesis. Cancer Cell 2006;10:437–49.
22. Jonkers J, Meuwissen R, van der Gulden H, Peterse H, van der Valk M, Berns A. Synergistic tumor suppressor activity of BRCA2 and p53 in a conditional mouse model for breast cancer. Nat Genet 2001;29:418–25.
23. Marino S, Vooijs M, van Der Gulden H, Jonkers J, Berns A. Induction of medulloblastomas in p53-null mutant mice by somatic inactivation of Rb in the external granular layer cells of the cerebellum. Genes Dev 2000;14:994–1004.
24. Segrelles C, Ruiz S, Santos M, Martinez-Palacio J, Lara MF, Paramio JM. Akt mediates an angiogenic switch in transformed keratinocytes. Carcinogenesis 2004;25: 1137–47.
25. Irizarry RA, Hobbs B, Collin F, et al. Exploration, normalization, and summaries of high density oligonucleotide array probe level data. Biostatistics 2003;4:249–64.
26. Bolstad BM, Irizarry RA, Astrand M, Speed TP. A comparison of normalization methods for high density oligonucleotide array data based on variance and bias. Bioinformatics 2003;19:185–93.
27. Vaquerizas JM, Conde L, Yankilevich P, et al. GEPAS, an experiment-oriented pipeline for the analysis of microarray gene expression data. Nucleic Acids Res 2005;33:W616–20.
28. Saeed AI, Sharov V, White J, et al. TM4: a free, open-source system for microarray data management and analysis. Biotechniques 2003;34:374–8.
29. Wijnhoven SW, Speksnijder EN, Liu X, et al. Dominant-negative but not gain-of-function effects of a p53.R270H mutation in mouse epithelium tissue after DNA damage. Cancer Res 2007;67:4648–56.
30. Segrelles C, Ruiz S, Perez P, et al. Functional roles of Akt signaling in mouse skin tumorigenesis. Oncogene 2002;21:53–64.
31. DiGiovanni J, Bol DK, Wilker E, et al. Constitutive expression of insulin-like growth factor-1 in epidermal basal cells of transgenic mice leads to spontaneous tumor promotion. Cancer Res 2000;60:1561–70.
32. Mason JM, Morrison DJ, Basson MA, Licht JD. Sprouty proteins: multifaceted negative-feedback regulators of receptor tyrosine kinase signaling. Trends Cell Biol 2006;16:45–54.
33. Bader AG, Kang S, Zhao L, Vogt PK. Oncogenic PI3K deregulates transcription and translation. Nat Rev Cancer 2005;5:921–9.
34. Cully M, You H, Levine AJ, Mak TW. Beyond PTEN mutations: the PI3K pathway as an integrator of multiple inputs during tumorigenesis. Nat Rev Cancer 2006;6:184–92.
35. Vivanco I, Sawyers CL. The phosphatidylinositol 3-kinase AKT pathway in human cancer. Nat Rev Cancer 2002;2:489–501.
36. Segrelles C, Lu J, Hammann B, et al. Deregulated activity of Akt in epithelial basal cells induces spontaneous tumors and heightened sensitivity to skin carcinogenesis. Cancer Res 2007;67:10879–88.
37. Altomare DA, Testa JR. Perturbations of the AKT signaling pathway in human cancer. Oncogene 2005;24: 7455–64.
38. Bellacosa A, Kumar CC, Di Cristofano A, Testa JR. Activation of AKT kinases in cancer: implications for therapeutic targeting. Adv Cancer Res 2005;94:29–86.
39. Segrelles C, Moral M, Lara MF, et al. Molecular determinants of Akt-induced keratinocyte transformation. Oncogene 2006;25:1174–85.
40. Bolontrade MF, Stern MC, Binder RL, Zenklusen JC, Gimenez-Conti IB, Conti CJ. Angiogenesis is an early event in the development of chemically induced skin tumors. Carcinogenesis 1998;19:2107–13.
41. Ziegler A, Jonason AS, Leffell DJ, et al. Sunburn and p53 in the onset of skin cancer. Nature 1994;372:773–6.
42. Greenhalgh DA, Wang XJ, Donehower LA, Roop DR. Paradoxical tumor inhibitory effect of p53 loss in transgenic mice expressing epidermal-targeted v-rasHa, v-fos, or human transforming growth factor α. Cancer Res 1996;56:4413–23.
43. Wang XJ, Greenhalgh DA, Jiang A, et al. Expression of a p53 mutant in the epidermis of transgenic mice accelerates chemical carcinogenesis. Oncogene 1998;17: 35–45.
44. Blanpain C, Fuchs E. Epidermal stem cells of the skin. Annu Rev Cell Dev Biol 2006;22:339–73.
45. Zhou Z, Flesken-Nikitin A, Nikitin AY. Prostate cancer associated with p53 and Rb deficiency arises from the stem/progenitor cell-enriched proximal region of prostatic ducts. Cancer Res 2007;67:5683–90.
46. Liu Y, Lyle S, Yang Z, Cotsarelis G. Keratin 15 promoter targets putative epithelial stem cells in the hair follicle bulge. J Invest Dermatol 2003;121:963–8.
47. Leis H, Segrelles C, Ruiz S, Santos M, Paramio JM. Expression, localization, and activity of glycogen synthase kinase 3β during mouse skin tumorigenesis. Mol Carcinog 2002;35:180–5.
48. Ferby I, Reschke M, Kudlacek O, et al. Mig6 is a negative regulator of EGF receptor-mediated skin morphogenesis and tumor formation. Nat Med 2006;12:568–73.
49. Sordella R, Bell DW, Haber DA, Settleman J. Gefitinib-sensitizing EGFR mutations in lung cancer activate anti-apoptotic pathways. Science 2004;305:1163–7.
50. Shaw AT, Meissner A, Dowdle JA, et al. Sprouty-2 regulates oncogenic K-ras in lung development and tumorigenesis. Genes Dev 2007;21:694–707.
51. Toussaint-Smith E, Donner DB, Roman A. Expression of human papillomavirus type 16 E6 and E7 oncoproteins in primary foreskin keratinocytes is sufficient to alter the expression of angiogenic factors. Oncogene 2004;23:2988–95.